A Letters Journal Exploring the Frontiers of Physics

March 2019

EPL, **125** (2019) 68003 www.epljournal.org
doi: 10.1209/0295-5075/125/68003

Emergence of Goldstone excitations in stress correlations of glass-forming colloidal dispersions

Florian Vogel[1], Annette Zippelius[2(a)] and Matthias Fuchs[1(b)]

[1] *University of Konstanz - D-78457 Konstanz, Germany*
[2] *University Göttingen - D-37077 Göttingen, Germany*

received 8 January 2019; accepted in final form 14 March 2019
published online 26 April 2019

PACS 81.05.Kf – Glasses (including metallic glasses)
PACS 62.20.-x – Mechanical properties of solids
PACS 82.70.Dd – Colloids

Abstract – We compute the dynamic correlations of the nonlocal shear stress at the liquid to glass transition in colloidal dispersions. Whereas Eshelby's elastic pattern is recovered independently of the dynamics, the Goldstone modes of the colloidal glass are diffusive, $\omega = -iDq^2$, because the transverse momentum is not conserved —excluding propagating transverse sound. Precursors of both, the Goldstone modes and the long-ranged, anisotropic stress correlations, can be observed in the colloidal fluid. The slow diffusive mode dominates the dynamics in the supercooled liquid for wave numbers $q\xi \gg 1$ with a correlation length $\xi \propto \tau^{1/2}$ which grows like the square root of the relaxation time τ. Time- and space-dependent stress correlations are anisotropic, decaying like r^{-5}. These results are derived within a hydrodynamic theory, generalising Maxwell's model to finite wave numbers, after the dynamics has been decomposed into potentially slow modes, associated with the order parameter, and fast microscopic degrees of freedom. Alternatively, hydrodynamic equations, closed by constitutive laws, can be used to predict the linear response of stress to an applied shear flow.

Introduction. – In the simplest theory of the glass transition, due to Maxwell [1], the transition is characterized not only by a divergence of the relaxation time τ but also, simultaneously, by the rigidity which the system develops with respect to shear [2–7]. More generally, the glass is considered an amorphous solid, exhibiting isotropic elasticity, implying long-ranged, anisotropic strain correlations. These correlations are a direct consequence of elasticity theory, were first discussed in detail by Eshelby [8], and have been seen in a variety of experiments [9–12] and simulations [13,14]. They also lay the basis for elastoplastic models of yielding in amorphous materials [15–18]. Two natural questions then arise: Can we see precursors of the elastic phenomena in the supercooled liquid, provided the relaxation time is large? And second, considering that dynamical Goldstone modes generally accompany long-ranged elastic correlations: Are there Goldstone modes in glass, and how do they emerge in the supercooled liquid upon approaching the glass transition? Maxwell partially answered the first question, arguing that a fluid behaves like an elastic solid on timescales short compared to τ. We went further and showed [19,20] that there are not only long-lived but also long-ranged correlations of the shear stress. In a Newtonian fluid, these are characterized by a correlation length $\xi \propto \tau$, which diverges at the glass transition. We showed that the coupling of the shear stress to a conserved quantity, the transverse momentum, is responsible for the slow decay in time and space of the stress autocorrelation.

Here we address the second question on Goldstone modes in an archetypical soft glassy material. More specifically, we consider a colloidal suspension, in which momentum conservation does not hold. Nevertheless, the coupling of the shear stress to tranverse velocity fluctuations has to be taken into account, in order to recover the elasticity of the glass and to obtain the correct long-lived and long-ranged correlations in the supercooled liquid. We argue that transverse velocity fluctuations can be regarded as order parameter fluctuations for the emergence of shear rigidity. We know that correlations of the tranverse displacement $\mathbf{u}^{\perp}(\mathbf{q})$ are long-ranged in the solid and

(a) E-mail: annette@theorie.physik.uni-goettingen.de
(b) E-mail: matthias.fuchs@uni-konstanz.de

therefore separate its dynamic fluctuations, or rather the time derivative, $\mathbf{v}^\perp(\mathbf{q}) = \boldsymbol{\partial}_t \mathbf{u}^\perp(\mathbf{q})$, from the fast degrees of freedom which are approximated by a single relaxation time *à la* Maxwell. The breaking of momentum conservation due to the solvent has important consequences: The Goldstone modes of the solid are diffusive instead of tranverse sound and the correlation length in the supercooled fluid obeys $\xi \propto \tau^{1/2}$.

Unified description. – The shear stress correlations in glass-forming systems are studied in a unified description encompassing molecular and colloidal fluids. We consider N particles with positions $\{\mathbf{r}\}_i^N$ and momenta $\{\mathbf{p}\}_i^N$ (or equivalently velocities $\mathbf{v}_i = \mathbf{p}_i/m$ for identical masses m) in suspension. The state of the system is specified by the N-particle phase-space distribution $\varrho(\Gamma, t) = \varrho(\{\mathbf{r}\}_i^N, \{\mathbf{p}\}_i^N, t)$ at fixed temperature T and volume V, whose time evolution is given by the Fokker-Planck equation $\partial_t \varrho = \Omega \varrho$ with

$$\Omega(\Gamma) = -\sum_i \left(\frac{\mathbf{p}_i}{m} \frac{\partial}{\partial \mathbf{r}_i} + \mathbf{F}_i \frac{\partial}{\partial \mathbf{p}_i} \right) + \sum_{i,j} \boldsymbol{\zeta}_{ij} \frac{\partial}{\partial \mathbf{p}_i} \left(k_B T \frac{\partial}{\partial \mathbf{p}_j} + \frac{\mathbf{p}_j}{m} \right). \quad (1)$$

The dynamic model includes the Newtonian limit $\boldsymbol{\zeta} = 0$, the overdamped limit, where inertial effects can be neglected, and possibly hydrodynamic interactions, when $\boldsymbol{\zeta}$ depends on the coordinates of the particles [21]. We discuss first the simplest case without hydrodynamic interactions, so that $\boldsymbol{\zeta}_{ij}$ is independent of position, constant, and diagonal: $\boldsymbol{\zeta}_{ij} = \zeta_0 \delta_{ij} \mathbf{1}$; see the appendix for further details.

The dynamics of the particles is captured in correlation functions defined as [22]

$$\langle A(t)^* B \rangle = \int \mathrm{d}\Gamma A^* e^{\Omega t} B \varrho_{\mathrm{eq}}, \quad (2)$$

where the integral extends over the whole phase space and ϱ_{eq} is the canonical Gibbs-Boltzmann distribution. We will exploit that the system is homogeneous, isotropic, and achiral, and that detailed balance holds [22]. We are interested in the response to an applied shear and hence focus on the autocorrelation of the shear stress,

$$C_\sigma(\mathbf{q}, t) = \frac{1}{V k_B T} \langle \sigma_{xy}(\mathbf{q}, t)^* \sigma_{xy}(\mathbf{q}) \rangle. \quad (3)$$

Here σ_{xy} stands for any off-diagonal element of the stress tensor, consisting of a kinetic and a potential contribution. For the latter we use the Irving-Kirkwood expression. Note that the full dependence on the direction of $\mathbf{q}$ is kept —in contrast to Maxwell's simple model and also in contrast to refs. [23,24], where the force correlations were studied. In the main part of the paper, we specialise to an incompressible system to simplify the discussion, but briefly comment on the effects of compressibility in the appendix.

Zwanzig-Mori decomposition of stress autocorrelation. – We know from previous work [19,20] that slow dynamics enters stress correlations, invalidating the Maxwell model and giving rise to long-range spatial correlations. In suspensions, the total momentum is not conserved due to frictional forces. However, slow dynamics can arise also due to order parameter fluctuations near a phase transition [25]. We expect that in the solid phase the correlations of the transverse displacement are long-ranged. It is our aim to follow the dynamics through the transition from the fluid into the glassy state and hence we include the transverse displacement or rather its time-derivative $\mathbf{v}^\perp(\mathbf{q}) = \boldsymbol{\partial}_t \mathbf{u}^\perp(\mathbf{q})$ into our set of slow variables —even though it is not conserved. The velocity field of N point particles is given by $\mathbf{v}(\mathbf{q}) = \sum_i \mathbf{v}_i e^{-i\mathbf{q}\cdot\mathbf{r}_i}$ and its transverse part by $\mathbf{v}^\perp(\mathbf{q}) = \mathbf{q} \times (\mathbf{v}(\mathbf{q}) \times \mathbf{q})/q^2$. The autocorrelation, $\langle \mathbf{v}^\perp(\mathbf{q}, t)^* \mathbf{v}^\perp(\mathbf{q}) \rangle = (\mathbf{1} - \frac{\mathbf{q}\mathbf{q}}{q^2}) K_q^\perp(t)$, has been computed by Hess and Klein [26], using projection operator techniques and linear response. In the long-wavelength limit, they found

$$K_q^\perp(s) = \frac{n k_B T}{snm + q^2 G_0^\perp(s) + n\zeta_0}. \quad (4)$$

Here, $G_0^\perp(s)$ denotes the generalised viscosity or shear modulus and the convention $C(s) = \int_0^\infty \mathrm{d}t e^{-st} C(t)$ is used, with s the Laplace frequency.

Defining the projector onto the transverse velocity field $\mathcal{P} = \frac{m}{N k_B T} \mathbf{v}^\perp(\mathbf{q}) \rangle \cdot \langle \mathbf{v}^\perp(\mathbf{q})^*$, we decompose the dynamics of the stress correlations into the subspace spanned by $\mathcal{P}$ and the rest, in complete analogy to ref. [19]. Furthermore, we consider the generalized hydrodynamic regime (index "GH") of smooth fluctuations, where only the leading orders in q in memory kernels need to be kept. Thereby we concentrate on the far-field correlations. We find for the Laplace transform of the stress autocorrelation the identical result as in [19,20]

$$C_\sigma^{\mathrm{GH}}(\mathbf{q}, s) = G_0^\perp(s) + (P(\mathbf{q}) - 1) \frac{q^2 (G_0^\perp(s))^2}{n k_B T} K_q^\perp(s). \quad (5)$$

Here the angular dependence is contained in $P(\mathbf{q}) = \left(4 \frac{q_x^2 q_y^2}{q^4} + \frac{q_z^2}{q^2}\right)$. The frictional forces, which explicitly break momentum conservation, are reflected only in the velocity correlations $K_q^\perp(s)$.

Generalised Maxwell model. – Once the slow dynamics has been displayed explicitly, we approximate the remaining fast dynamics, entailed in $G_0^\perp(s)$, in the spirit of Maxwell by a single relaxation time τ:

$$G_0^\perp(s) \approx G^{\mathrm{gM}}(s) = \frac{G_\infty \tau}{1 + s\tau}. \quad (6)$$

The glass transition is signaled by a divergence of τ, which we do not specify explicitly. The model is defined by entering eq. (6) into eqs. (4) and (5) and is termed generalized Maxwell (index "gM") because there is a crucial

difference to the classic Maxwell model [1]. The generalized model first isolates the slow modes, and then approximates the remaining fluctuating forces. Maxwell's model, in contrast, approximates the correlations of the full stress fluctuations.

The single relaxation time approximation for $G_0^\perp(s)$ completes our description of the colloidal fluid to glass transition, which will be analysed in detail in the following sections. The formal development is rather similar to the Newtonian case. The generalised Maxwell model is identical; however, for the colloidal case the separation into fast and slow dynamics requires the proximity to the glass transition. The breaking of momentum conservation causes important differences on the dynamic spectra of both, the fluid and the glass, compared to the Newtonian case.

Elasticity in the glassy state. We first discuss stress correlations in the glassy state, where the relaxation time τ is infinite, so that $G^{\rm gM}(s) = \frac{G_\infty}{s}$ and the tranverse velocity correlation is given by

$$K_q^{\perp,{\rm gM}}(s) = \frac{nk_BT}{snm + \frac{q^2G_\infty}{s} + n\zeta_0}, \qquad \text{for } \frac{1}{\tau} = 0. \tag{7}$$

Hence in the low-frequency limit, it is proportional to s in agreement with time persistent correlations of the transverse displacement $\mathbf{u}^\perp(\mathbf{q})$. Inserting the above result for $K_q^\perp$ into eq. (5), we find time persistent correlations for the shear stress as well. These contributions can be isolated as the leading order in the limit $s \to 0$:

$$\lim_{s\to 0} s\, C_\sigma^{\rm gM}(\mathbf{q},s) = C_\sigma^\infty(\mathbf{q}) = G_\infty\left(\frac{q_z^2}{q^2} + 4\frac{q_x^2q_y^2}{q^4}\right). \tag{8}$$

The generalised Maxwell model correctly predicts the anisotropic stress correlations in an isotropic elastic solid, which have been discussed extensively in recent literature and already by Eshelby [8,15]. Furthermore, the static elasticity is independent of the underlying dynamics. It is the same for Newtonian and colloidal dynamics. This is of course to be expected, but note that the above result can only be reproduced, if the coupling to transverse velocity fluctuations is correctly taken into account.

The dynamics in the glassy phase is sensitive to the underlying dynamic model. In the underdamped limit, $\zeta_0/m \ll s$, we recover undamped sound modes as for the Newtonian glass [20]. In the strongly damped limit, $\zeta_0/m \gg s$, we obtain (recall that $1/\tau = 0$)

$$\begin{aligned}\Delta C_\sigma^{\rm gM}(\mathbf{q},s) &:= C_\sigma^{\rm gM}(\mathbf{q},s) - \frac{1}{s}C_\sigma^\infty(\mathbf{q}) \\ &= G_\infty\left(\frac{q_x^2+q_y^2}{q^2} - 4\frac{q_x^2q_y^2}{q^4}\right)\frac{\zeta_0}{s\zeta_0 + q^2G_\infty/n}.\end{aligned} \tag{9}$$

Equation (9) displays a diffusive pole, $s = -q^2D$ with $D = G_\infty/(n\zeta_0)$, implying slow dynamics in the hydrodynamic limit. In the left panel of fig. 1, we show the Fourier

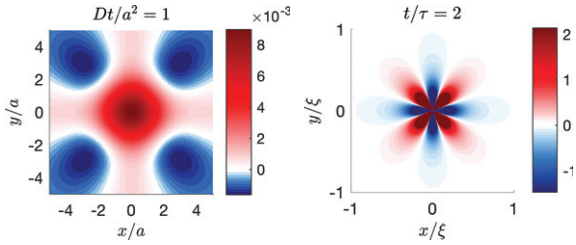

Fig. 1: Color scale contour plots of shear stress correlations. Left panel: Goldstone mode contribution $\Delta C_\sigma^{\rm gM}(\mathbf{r},t)\xi^3/G_\infty$ (see eq. (9)) in glass at rescaled time $tD/a^2 = 1$ with $D = G_\infty/(n\zeta_0)$ and microscopic length a. Right panel: rescaled stress $\frac{\xi^3}{G_\infty}C_\sigma^{\rm gM}(\mathbf{r},t)$ of a colloidal fluid in the x-y plane at $z = 0$ and $t/\tau = 2$ (with divergence $\propto r^{-3}$ for $r \to 0$ cutoff at $r/\xi = 0.28$); see eq. (13).

back-transformation of eq. (9) in real space for rescaled time $t = Da^2$ with a microscopic length a.

We interpret this slow mode as a Goldstone excitation due to the long-range correlations of the transverse displacement [27]. In our approach, this slow mode is a straightforward result of the microscopic dynamics and the generalised Maxwell model. For its interpretation, it is nevertheless useful to invoke the elastic free energy of an amorphous, isotropic solid $F = \mu/2\int {\rm d}^dq q^2\mathbf{u}^\perp(\mathbf{q})\cdot\mathbf{u}^\perp(-\mathbf{q})$ (incompressible limit assumed) which gives rise to the above stress correlations (eq. (8)). For purely relaxational dynamics, one finds

$$n\zeta_0\partial_t\mathbf{u}^\perp(\mathbf{q}) = -\frac{\delta F}{\delta\mathbf{u}^\perp(-\mathbf{q})} = -\mu q^2\mathbf{u}^\perp(\mathbf{q}) \tag{10}$$

in agreement with the dispersion predicted from eq. (9), if we identify the shear modulus $\mu = G_\infty$. The predicted diffusive Goldstone mode should be observable in experiments, which record particle trajectories to sample the displacement fluctuations [28].

Goldstone modes in general are expected in a phase with a spontaneously broken continuous symmetry. In the ideal glass it is the translational symmetry of the Hamiltonian which is broken, as signaled by nonzero expectation values of the local density in a pure state: $\langle e^{i\mathbf{q}\cdot\mathbf{r}_i}\rangle_p \neq 0$. The particles are strictly localised with finite thermal excursions around their preferred positions. In contrast to crystalline solids, the translational symmetry in glasses is broken on a local level only. Macroscopic observables exhibit the full translational invariance of the underlying model so that the global density vanishes: $\frac{1}{N}\sum_i\langle e^{i\mathbf{q}\cdot\mathbf{r}_i}\rangle_p = 0$ for all nonzero $\mathbf{q}$. To see the locally broken translational symmetry one has to resort to macroscopic correlations, such as the time persistent part of the van Hove scattering function [29–31].

Relaxation in the fluid phase. We consider only the overdamped limit, which is achieved by ignoring the inertial terms (setting $m = 0$) but allowing for the full range

of $s\tau$:

$$C_\sigma^{\rm GH}(\mathbf{q},s) = G^{\rm GH}(s)\left[1+\big(P(\mathbf{q})-1\big)\frac{q^2G_\infty\tau}{n\zeta_0(1+s\tau)+q^2G_\infty\tau}\right]. \tag{11}$$

For a nontrivial q-dependence to survive we need finite values of $q^2\frac{G_\infty\tau}{n\zeta_0}$. For large damping, $q\sqrt{\tau}$ has to be large as well. In the glass this is trivially fulfilled, because τ is infinite (see eq. (9)). For finite τ, this precludes the true hydrodynamic limit $q\to 0$; nevertheless the rapid increase of τ near the glass transition allows one to choose small wave numbers as long as $q^2=\mathcal{O}(\zeta_0/\tau)$, which is always possible sufficiently close to the glass transition.

The frequency-dependent spectra, $C'_\sigma(\mathbf{q},\omega) - iC''_\sigma(\mathbf{q},\omega) = -i\omega C_\sigma(\mathbf{q},s=-i\omega)$, can be measured in rheological experiments on colloidal suspensions, for which the large damping limit should apply. The spectra strongly depend on the direction of $\mathbf{q}$. We pick two representative ones: $\mathbf{q}=(q,0,0)$ and $\mathbf{q}=(q,q,0)/\sqrt{2}$, all others can be obtained via superposition. For the latter case, the spectra reduce to the well-known result of Maxwell. The long-range stress correlations are seen in the former case ($\mathbf{q}=(q,0,0)$), for which the spectra are given by

$$C_\sigma^{\rm gM\prime}(q,\omega) = G_\infty\frac{\omega^2\tau^2}{(q^2\xi^2+1)^2+\omega^2\tau^2}, \tag{12a}$$

$$C_\sigma^{\rm gM\prime\prime}(q,\omega) = G_\infty\frac{\omega\tau(q^2\xi^2+1)}{(q^2\xi^2+1)^2+\omega^2\tau^2}. \tag{12b}$$

Here we have introduced the correlation length $\xi^2=\frac{G_\infty\tau}{n\zeta_0}$, such that the spectra obey scaling: $C_\sigma^{\rm gM\prime\prime}(q,\omega)=F(q\xi,\omega\tau)$ and similarly for C'. Note that the divergence of the correlation length, $\xi\propto\sqrt{\tau}$, differs from the Newtonian case, where we found $\xi\propto\tau$ [19]. Both correlation lengths are seen in strain correlations also [14], which suggests that a generalized Hookean relation could be established in viscoelastic liquids. The spectra are shown in fig. 2 for several values of $q\xi$. For sufficiently large $q\xi>1$, the peak in the loss spectrum is determined by $\omega_{\max}\tau\sim q^2\xi^2$ and the diffusive mode identified in eq. (9) can be observed. On the other hand, for $q\xi\to 0$, Maxwell's relaxation with $\omega_{\max}\tau\sim 1$ is recovered.

Time- and space-dependent correlations. The long-ranged, anisotropic stress correlations are clearly seen in the time- and space-dependent correlations. In the overdamped limit, the Laplace back-transformation of eq. (11) can be done exactly

$$C_\sigma^{\rm gM}(\mathbf{q},t)/G^{\rm gM}(t) = P(\mathbf{q}) + (1-P(\mathbf{q}))e^{-q^2Dt}. \tag{13}$$

At long times, the stress correlations are dominated by the first term in eq. (13), implying for the space-dependent correlation

$$C_\sigma^{\rm gM}(\mathbf{r},t) = G_\infty e^{-t/\tau}P(\mathbf{r}), \tag{14}$$

viz. Eshelby's pattern decaying with the Maxwell relaxation time τ. In general, the space-dependent correlations are determined by the ratio r^2/t and can be written

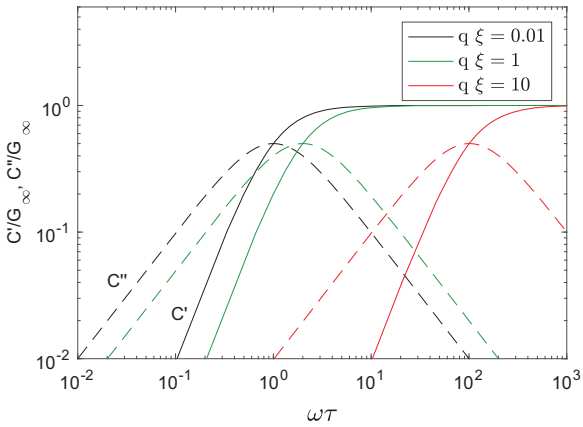

Fig. 2: Shear stress spectra of the generalized Maxwell model for fixed wave vector directed tangential to the stress-plane, *viz.* $\mathbf{q}=(q,0,0)$ for σ_{xy}. The storage, $C_\sigma^{\rm gM\prime}(q,\omega)$, and loss part, $C_\sigma^{\rm gM\prime\prime}(q,\omega)$, given in eq. (12), as functions of the rescaled frequency $\omega\tau$ are shown as solid and dashed lines, respectively. The wave vector magnitude varies as given in the legend.

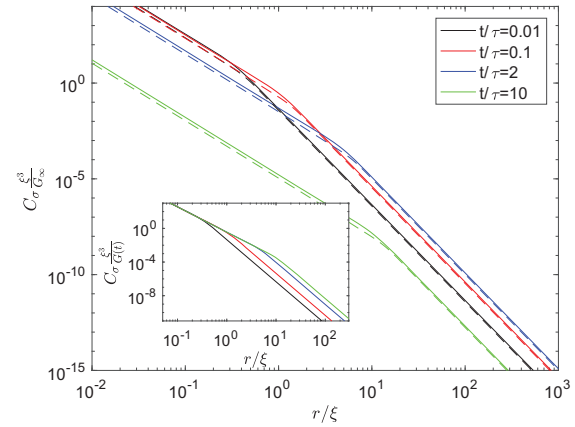

Fig. 3: Stress profiles $\frac{\xi^3}{G_\infty}C_\sigma^{\rm gM}(\mathbf{r},t)$ along the diagonal (solid) and along the x-axis (dashed line, absolute value shown) in the $(z=0)$-plane for rescaled times given in the legend. The inset verifies the collapse of the rescaled profiles $C_\sigma^{\rm gM}(\mathbf{r},t)/G^{\rm gM}(t)$ onto the Eshelby pattern at short distances, see eq. (14).

as $C_\sigma^{\rm gM}(\mathbf{r},t)/G^{\rm gM}(t)=\frac{1}{r^3}\mathcal{F}(\mathbf{r}/\sqrt{t})$. The asymptotics for large r can be computed following ref. [15]; the leading term for $r^2\gg Dt$ is explicitly given by

$$\lim_{r\to\infty} r^5 C_\sigma^{\rm gM}(\mathbf{r},t)/G^{\rm gM}(t) = \frac{3Dt}{\pi}\left(1-5\frac{x^2+y^2}{r^2}+35\frac{x^2y^2}{r^4}\right). \tag{15}$$

Hence stress correlations in the fluid are always strongly anisotropic, decaying like r^{-5} for the largest r. At $r^2/t=D$ there is a crossover to r^{-3}, which is seen best along cuts in the x-y plane. Two profiles, $C_\sigma^{\rm gM}(x=y,t)$ and $C_\sigma^{\rm gM}(x,y=0,t)$, shown in fig. 3, clearly display the asymptotic decay as well as the crossover. In the inset we show the same profiles normalized by $G^{\rm gM}(t)$; these functions displays the universal Eshelby pattern of eq. (14) for all t/τ, so that the data collapse for small distances

$r^2 \ll Dt$. Eshelby's power ($\sim r^{-3}$) and the diffusive scaling function $\mathcal{F}(\mathbf{r}/\sqrt{t})$ of the pattern explain the power-law $C_\sigma^{\mathrm{gM}}(\mathbf{r},t) \to t/r^5$ for short times, which is given in eq. (15). If the system had a nonzero, but small compressibility, κ_T, the asymptotic decay r^{-5} would be cut off [32] at the scale $r^2/t = 1/(n\zeta_0\kappa_T)$. We also show a characteristic contour plot in the right panel of fig. 1 for $t/\tau = 2$. The overall magnitude of the contour plot is determined by $e^{-t/\tau}$ (see scale), but apart from that, all patterns are rather similar, clearly displaying a fourfold angular variation.

Hydrodynamic equations. – In rheology contexts, stress correlations are often described in hydrodynamic laws closed by constitutive equations [33]. The generalized Maxwell model for dispersion rheology can easily be reformulated in this manner.

The total velocity field of the particles in the laboratory frame is decomposed into the (incompressible) solvent velocity field $\mathbf{v}^{\mathrm{ext}}(\mathbf{r},t)$, which we assume to be externally prescribed, and the particles' velocity $\mathbf{v}(\mathbf{r},t)$ moving relative to the solvent. For simplicity, we consider the colloidal system to be incompressible, which requires that its velocity field is purely transverse, $\nabla\cdot\mathbf{v}(\mathbf{r},t) = 0$. The gradient tensor of the total velocity field then is the sum of terms arising from the solvent and from the particles,

$$\boldsymbol{\kappa}(\mathbf{r},t) = \left[\nabla\mathbf{v}(\mathbf{r},t) + \nabla\mathbf{v}^{\mathrm{ext}}(\mathbf{r},t)\right]^T, \tag{16a}$$

where only the symmetrized gradient will be required in linear response: $\bar{\boldsymbol{\kappa}}(\mathbf{r},t) = \frac{1}{2}\left(\boldsymbol{\kappa}(\mathbf{r},t) + \boldsymbol{\kappa}(\mathbf{r},t)^T\right)$. The constitutive equation for the stress, $\boldsymbol{\sigma}^{\mathrm{gM}}(\mathbf{r},t)$, is built on Maxwell's insight in glassy relaxation:

$$(1+\tau\partial_t)\boldsymbol{\sigma}^{\mathrm{gM}}(\mathbf{r},t) = 2G_\infty\tau\,\bar{\boldsymbol{\kappa}}(\mathbf{r},t). \tag{16b}$$

It contains the total velocity field because stresses are generated from the inhomogeneity of the complete flow including the solvent and the particles. Stresses relax with a finite relaxation time τ in fluid states. The equations are closed by the hydrodynamic force-balance equation which is valid in Langevin systems. It yields the equation for the particles' velocity field $\mathbf{v}(\mathbf{r},t)$. The forcing from the stress inhomogeneities is opposed to the Stokesian friction on the particles from the solvent, characterized by ζ_0,

$$mn\dot{\mathbf{v}}(\mathbf{r},t) + n\zeta_0\mathbf{v}(\mathbf{r},t) = \nabla\cdot\left(\boldsymbol{\sigma}^{\mathrm{gM}}(\mathbf{r},t) - p(\mathbf{r},t)\mathbf{1}\right). \tag{16c}$$

The underdamped case is included by the inertial term. The coupling of viscoelastic stresses and the motion of the particles in eq. (16) leads to a spatially nonlocal differential equation for the stress.

Solving eq. (16) for the flow-induced stress reproduces the linear response relation in the incompressible case. The proof proceeds in Fourier space by calculation of $\boldsymbol{\sigma}^{\mathrm{gM}}(\mathbf{q},\omega)$ for an external shear perturbation $\boldsymbol{\kappa}^{\mathrm{ext}}(\mathbf{q},\omega) = \dot\gamma(\mathbf{q},\omega)\hat{\mathbf{x}}\hat{\mathbf{y}}$. The stress correlation function then is the Green's function $\mathrm{C}_\sigma^{\mathrm{gM}}(\mathbf{q}, s=-i\omega) = \sigma_{xy}^{\mathrm{gM}}(\mathbf{q},\omega)/\dot\gamma(\mathbf{q},\omega)$. For the dynamics described by the Fokker-Planck operator of eq. (1), there is an additional contribution to the stress due to the frictional forces, so that the total stress is given by $\boldsymbol{\sigma}_{xy}(\mathbf{r},t) = \boldsymbol{\sigma}_{xy}^{\mathrm{gM}}(\mathbf{r},t) + \eta_\infty\,\dot\gamma(\mathbf{r},t)$. The high-frequency viscosity is determined by momentum relaxation, which is fast in the overdamped case.

Conclusions and outlook. – We have presented a unified description of nonuniform stress correlations at the glass transition. Our approach is based on a decomposition of stress fluctuations into a contribution which becomes long-lived and long-ranged at the glass transition and microscopic degrees of freedom which have been approximated by a single relaxation time τ, whose divergence signals the glass transition. The glassy state is characterized by time persistent stress correlations, which display the familiar Eshelby pattern. As expected, the elasticity of the glass is independent of the dynamics —be it Newtonian or overdamped. We have furthermore argued that in the glassy state the translational symmetry is spontaneously broken due to the localisation of particles at random positions. This spontaneous symmetry breaking gives rise to Goldstone modes, which are, however, very different for Newtonian dynamics with momentum conservation and overdamped dynamics, where momentum conservation is violated. Whereas in the former case the Goldstone excitations are propagating sound modes, they are diffusive in the colloidal glass. The frequency-dependent spectra, which are measured in experiments on colloidal glasses, hence should display diffusive peaks according to the dispersion $\omega = -iq^2\frac{G_\infty}{n\zeta_0}$. The long-range stress correlations in the glass give rise to precursors in the fluid close to the glass transition. The diffusive Goldstone mode can be observed in the supercooled liquid for $q\xi \gg 1$, where the correlation length $\xi \propto \sqrt{\tau}$ grows like the square root of the relaxation time. Space- and time-dependent correlations fall off as r^{-5}, crosssing over to r^{-3} at $r^2 = Dt$. For small but finite isothermal compressibility, κ_T, the algebraic decay is cut off at large $r^2/t \sim 1/\kappa_T$.

We neglected hydrodynamic interactions in the main part of our paper. Yet, we showed that momentum relaxation caused by local friction with the solvent is consistent with the build-up of elastic stresses. In the appendix, we argue that hydrodynamic interactions do not change the phenomena qualitatively because momentum relaxation can be assumed to remain fast even if solvent flows are included. Then hydrodynamic interactions solely renormalize the high-frequency parameters of our approach. Yet, a more detailed study, possibly building on field-theoretic models [34], especially of inhomogeneous and strong flows, would be worthwhile in future.

Appendix. – Details of derivations are given.

Methods. We sketch the derivation of eq. (5) starting from eq. (1). The formal steps follow the route to Newtonian systems [20] and can include hydrodynamic interactions straightforwardly. The time evolution of the velocity field $\mathbf{v}(\mathbf{q})$ is required. It follows from eq. (2) and is given

by $\partial_t\langle \mathbf{v}(\mathbf{q},t)^* B\rangle = \langle (\Omega^\dagger \mathbf{v}(\mathbf{q},t))^* B\rangle$ with [26]:

$$m\Omega^\dagger \mathbf{v}(\mathbf{q}) = \sum_i (-im\mathbf{q}\cdot\mathbf{v}_i)\mathbf{v}_i e^{-i\mathbf{q}\cdot\mathbf{r}_i} + \sum_i \mathbf{F}_i e^{-i\mathbf{q}\cdot\mathbf{r}_i} - \sum_{i,j}\mathbf{v}_i\boldsymbol{\zeta}_{ij}e^{-i\mathbf{q}\cdot\mathbf{r}_j} = -i\mathbf{q}\cdot\boldsymbol{\sigma}(\mathbf{q}) + \mathbf{F}^{(F)}(\mathbf{q}). \tag{A.1}$$

The first two terms can be identified with the kinetic and potential contribution to the stress tensor, respectively. The third term is due to the frictional forces and breaks momentum conservation explicitly. Both fields, stresses and frictional forces, appear in the following.

Applying the Zwanzig-Mori approach using the operator $\mathcal{Q} = 1 - \mathcal{P}$ projecting onto the complement of the transverse velocities, the explicit decomposition of the dynamic stress autocorrelation in eq. (3) into potentially slow dynamics yields the following exact result:

$$C_\sigma(\mathbf{q},s) = M_{xyxy}(\mathbf{q},s) - \left((q_x^2+q_y^2) - 4\frac{q_x^2q_y^2}{q^2}\right)\frac{\left((G_q^\perp(s))^2 + (E_q^{(2)}(s))^2\right)}{nk_BT}K_q^{\perp,\mathrm{ZM}}(s). \tag{A.2}$$

(The superscript $^{\mathrm{ZM}}$ on the current correlation function indicates that the limit of generalized hydrodynamics has not yet been taken.) Here, eq. (A.1) was used and leads to the following kernels which are built with the reduced resolvent, $R'(s)$, defined via $R'(s) = \mathcal{Q}(s-\mathcal{Q}\Omega\mathcal{Q})^{-1}\mathcal{Q}$ [35]: First, the shear modulus arises which generalizes the shear viscosity to finite frequency and wave number,

$$G_q^\perp(s) = \frac{1}{Vk_BT}\langle(\mathcal{Q}\sigma_{xy}(q\hat{\mathbf{y}}))^* R'(s)(\mathcal{Q}\sigma_{xy}(q\hat{\mathbf{y}}))\rangle. \tag{A.3}$$

In order to be specific, the wave vector was chosen along the y-axis, so that v_x is a transverse velocity and σ_{xy} a shear stress. Then, another kernel couples shear stresses, and a third one couples stresses and frictional forces:

$$M_{xyxy}(\mathbf{q},s) = \frac{1}{Vk_BT}\langle(\mathcal{Q}\sigma_{xy}(\mathbf{q}))^* R'(s)(\mathcal{Q}\sigma_{xy}(\mathbf{q}))\rangle, \tag{A.4}$$

$$E_q^{(2)}(s) = \frac{i}{Vk_BTq}\langle(\mathcal{Q}\sigma_{xy}(q\hat{\mathbf{y}}))^* R'(s)(\mathcal{Q}F_x^{(F)}(q\hat{\mathbf{y}}))\rangle. \tag{A.5}$$

In the derivation of eq. (A.2), we used isotropy and inversion symmetry which imply $\langle\boldsymbol{\sigma}(\mathbf{q},t)^*\mathbf{F}^{(F)}(\mathbf{q})\rangle = -\langle\boldsymbol{\sigma}(-\mathbf{q},t)^*\mathbf{F}^{(F)}(-\mathbf{q})\rangle$, valid for the full and the reduced dynamics [36]. The kernel arising in $E^{(2)}$ thus is linear in the wave vector for small $\mathbf{q}$. Additionally we used that detailed balance, valid close to equilibrium, gives $\langle\sigma_{\alpha\beta}(\mathbf{q},t)^*F_\gamma^{(F)}(\mathbf{q})\rangle = -\langle F_\gamma^{(F)}(\mathbf{q},t)^*\sigma_{\alpha\beta}(\mathbf{q})\rangle$. This also entered in the derivation of eq. (4), which was generalized to include hydrodynamic interactions by Hess and Klein [26]. They showed that the exact $K_q^{\perp,\mathrm{ZM}}(s)$ contains the shear modulus given in eq. (A.3) and that $n\zeta_0$ is replaced by the kernel $\zeta_q^\perp(s)$, which arises from the nonlocal friction forces,

$$\zeta_q^\perp(s) = \frac{1}{Vk_BT}\Big[k_BT\Big\langle\sum_{i,j}\zeta_{ij}^{xx}e^{iq(y_i-y_j)}\rangle - \langle(\mathcal{Q}F_x^{(F)}(q\hat{\mathbf{y}}))^* R'(s)(\mathcal{Q}F_x^{(F)}(q\hat{\mathbf{y}}))\Big\rangle\Big]. \tag{A.6}$$

In the main test, we studied eq. (A.2) only in the simplest case without hydrodynamic interactions, so that $\boldsymbol{\zeta}_{ij}$ is independent of position, constant, and diagonal: $\boldsymbol{\zeta}_{ij}(\{\mathbf{r}\}_i^N) = \zeta_0\delta_{ij}\mathbf{1}$. The fluctuating friction forces then vanish: $\mathcal{Q}\mathbf{F}^{(F)}(\mathbf{q}) = 0$. This reduces the stress-friction coupling to zero, $E_q^{(2)}(s) = 0$ and gives the instantaneous friction coefficient in eq. (4). Furthermore, we considered the generalized hydrodynamic (index "GH") regime of smooth fluctuations [37], where only the leading orders in q in memory kernels need to be kept, thereby concentrating on the far-field correlations. Then $M_{xyxy}(\mathbf{q},s) = G_0^\perp(s) + \mathcal{O}(q^2)$ can be used. With these approximations the results of eqs. (4), (5) are recovered.

Discussion of hydrodynamic interactions. In the general case with hydrodynamic interactions, the kernels eqs. (A.5), (A.6) contain the friction with the solvent and thus depend on the relaxation of the particle momentum. In the overdamped limit, understood as the limit of small frequency $s \to 0$, we anticipate that these kernels can be replaced by finite, frequency-independent values:

$$\zeta_q^\perp(s) \to \zeta_q^\perp \quad \text{and} \quad E_q^{(2)}(s) \to E_q^{(2)}. \tag{A.7}$$

All of our results are recovered, *if* we make the additional assumption that the generalized shear modulus in the overdamped limit, in contrast, still varies with frequency. Following Maxwell, we anticipate this because $G_0^\perp(s)$ is characterized by a relaxation time τ which grows beyond bounds at the glass transition. The precise limit is $s \to 0$ and $\tau \to \infty$ such that $s\tau$ is kept fixed. Additionally, the implicit assumption is required that all kernels remain finite for wavevector going to zero. Then, hydrodynamic interactions solely affect the behavior of the generalized shear modulus at high frequencies in eq. (A.2) and renormalize the friction coefficient ζ_0 to $\zeta_0^\perp$. Interestingly, starting from the overdamped limit itself, *viz.* the Smoluchowski equation, this separation of effects does not become so apparent [38].

Compressible case. Colloidal fluids are slightly compressible, because the (generalized) isothermal compressibility $\kappa_q^T = S_q/(nk_BT)$, with S_q the fluid structure factor, is small but finite [26]. It is expedient to verify that compression effects do not qualitatively affect the fluctuations and far-field pattern of the transverse deformations [20,32]. This requires to generalize the Zwanzig-Mori projector $\mathcal{P}$ to also include longitudinal

fluctuations, *viz.* $(1-\mathcal{Q}) = \mathcal{P} = (1/NS_q)\delta\varrho(\mathbf{q})\rangle\langle\delta\varrho(\mathbf{q})^* + (m/Nk_BT)\mathbf{v}(\mathbf{q})\rangle \cdot \langle\mathbf{v}(\mathbf{q})^*$. Longitudinal velocity fluctuations then couple into the shear stress and the r.h.s. of eq. (A.2) obtains the additional term:

$$-\frac{q_x^2 q_y^2}{q^2}\frac{((M_q^{\parallel(2)}(s))^2 + (E_q^{\parallel}(s))^2)}{nk_BT}K_q^{\parallel}(s) \qquad \text{(A.8)}$$

Here $K_q^{\parallel}(s)$ correlates the longitudinal velocities and can be taken from ref. [26]. The structural coupling kernel $M^{\parallel(2)}(q,s)$ was defined in ref. [20]. It becomes $M^{\parallel(2)}(q,s) \to 2G_0^{\perp}(s)$ in the hydrodynamic limit $q \to 0$. The frictional kernel is

$$E_q^{\parallel} = \frac{\left[\langle\sigma_{yy}^*(q\hat{\mathbf{y}})R'F_y^{(F)}(q\hat{\mathbf{y}})\rangle - \langle\sigma_{xx}^*(q\hat{\mathbf{y}})R'F_y^{(F)}(q\hat{\mathbf{y}})\rangle\right]}{Vk_BT(-iq)},$$

and reduces to $E^{\parallel}(q,s) \to 2E_0^{(2)}(s)$ for small wave vector. Equation (A.8) states that, because of $(m/k_BT)K_q^{\parallel}(s) \leq s\kappa_q^T/q^2$, a finite but small compressibility leads to small corrections; *e.g.*, the time evolution of the transient stress pattern in eq. (15) changes. While in the incompressible case it initially grows linearly with time, in the compressible case, it is built up by a diffusive longitudinal mode characterized by the (fast) compression diffusion coefficient $D_L = 1/(n\zeta_0\kappa_0^T)$. Because of the angular dependence, the rheological spectra given in eq. (12) and shown in fig. 2 are not affected. Also, hydrodynamic interactions again only renormalize the high-frequency behaviour.

REFERENCES

[1] Maxwell J. C., *Philos. Trans. R. Soc. A*, **157** (1867) 49.
[2] Lemaître A., *Phys. Rev. Lett.*, **113** (2014) 245702.
[3] Flenner E. and Szamel G., *Phys. Rev. Lett.*, **114** (2015) 025501.
[4] Wittmer J. P., Xu H. and Baschnagel J., *Phys. Rev. E*, **91** (2015) 022107.
[5] Saw S. and Harrowell P., *Phys. Rev. Lett.*, **116** (2016) 137801.
[6] Chowdhury S., Abraham S., Hudson T. and Harrowell P., *J. Chem. Phys.*, **144** (2016) 124508.
[7] Kriuchevskyi I., Wittmer J. P., Meyer M. and Baschnagel J., *Phys. Rev. Lett.*, **119** (2017) 147802.
[8] Eshelby J., *Proc. R. Soc. London A*, **241** (1957) 376.
[9] Desmond K. W. and Weeks E. R., *Phys. Rev. Lett.*, **115** (2015) 098302.
[10] Lin N. Y. C., Bierbaum M., Schall P., Sethna J. P. and Cohen I., *Nat. Mater.*, **15** (2016) 1172.
[11] Majmudar T. S. and Behringer R. P., *Nature*, **435** (2005) 1079.
[12] Illing B., Fritschi S., Hajnal D., Klix C. L., Keim P. and Fuchs M., *Phys. Rev. Lett.*, **117** (2016) 208002.
[13] Chattoraj J. and Lemaître A., *Phys. Rev. Lett.*, **111** (2013) 066001.
[14] Hassani M., Zirdehi E. M., Kok K., Schall P., Fuchs M. and Varnik F., *EPL*, **124** (2018) 18003.
[15] Picard G., Ajdari A., Lequeux F. and Bocquet L., *Eur. Phys. J. E*, **15** (2004) 371.
[16] Ferrero E. E., Martens K. and Barrat J.-L., *Phys. Rev. Lett.*, **113** (2014) 248301.
[17] Nicolas A., Rottler J. and Barrat J.-L., *Eur. Phys. J. E*, **37** (2014) 50.
[18] Nicolas A., Ferrero E. E., Martens K. and Barrat J.-L., *Rev. Mod. Phys.*, **90** (2018) 045006.
[19] Maier M., Zippelius A. and Fuchs M., *Phys. Rev. Lett.*, **119** (2017) 265701.
[20] Maier M., Zippelius A. and Fuchs M., *J. Chem. Phys.*, **149** (2018) 084502.
[21] Dhont J. K. G., *An Introduction to Dynamics of Colloids* (Elsevier, Amsterdam) 1996.
[22] Risken H., *The Fokker-Planck Equation* (Springer, Berlin) 1984.
[23] Evans D., *Phys. Rev. A*, **23** (1981) 2622.
[24] Semenov A. N., Farago J. and Meyer H., *J. Chem. Phys.*, **136** (2012) 244905.
[25] Hohenberg P. and Halperin B., *Rev. Mod. Phys.*, **45** (1977) 435.
[26] Hess W. and Klein R., *Adv. Phys.*, **32** (1983) 173.
[27] Mukhopadhyay S., Goldbart P. M. and Zippelius A., *Europhys. Lett.*, **67** (2004) 49.
[28] Klix C. L., Maret G. and Keim P., *Phys. Rev. X*, **5** (2015) 041033.
[29] Barrat J. L., Götze W. and Latz A., *J. Phys.: Condens. Matter*, **1** (1989) 7163.
[30] Goldbart P. and Goldenfeld N., *Phys. Rev. A*, **39** (1989) 1402.
[31] Ulrich S., Mao X., Goldbart P. and Zippelius A., *EPL*, **76** (2006) 677.
[32] Klochko L., Baschnagel J., Wittmer J. P. and Semenov A. N., *Soft Matter*, **14** (2018) 6835.
[33] Larson R. G., *The Structure and Rheology of Complex Fluids* (Oxford University Press, New York) 1999.
[34] Krüger M., Solon A., Démery V., Rohwer C. M. and Dean D. S., *J. Chem. Phys.*, **148** (2018) 084503.
[35] Forster D., *Hydrodynamic Fluctuations, Broken Symmetry, and Correlation Functions, Advanced Book Classics* (Perseus Books, New York) 1995.
[36] Vogel F., *Shear-stress correlation function and linear response in Langevin systems*, Bachelor thesis, Universität Konstanz, FB Physik (July 23, 2018).
[37] Götze W. and Latz A., *J. Phys.: Condens. Matter*, **1** (1989) 4169.
[38] Nägele G. and Dhont J. K. G., *J. Chem. Phys.*, **108** (1998) 9566.